MECHANISMS OF MOTION SHARPENING IN STEREOSCOPIC MOTION IN DEPTH

A thesis presented to the Graduate Faculty
of the New England College of Optometry in partial fulfillment
of the requirements for the degree of Master of Science

Jeff Ferrucci

April 2018

©Jeff Ferrucci
All rights reserved

The author hereby grants the New England College of Optometry permission to reproduce and to distribute publicly paper and electronic copies of the thesis document in whole or in part.

MECHANISMS OF MOTION SHARPENING IN STEREOSCOPIC MOTION IN DEPTH

Jeff Ferrucci

This manuscript has been read and accepted by the Thesis Examination Committee in satisfaction of the thesis requirement for the degree of Master of Science.

May 15, 2018
Date

Glen McCormack, O.D., Ph.D.
Graduate Faculty Advisor

Peter Bex, Ph.D.
Thesis Committee Member

Frank Thorn, Ph.D., O.D.
Thesis Committee Member

Frances Rucker, Dip. Opt. Optics., MSc., Ph.D., MCOptom., FAAO
Thesis Committee Member

May 15, 2018
Date

Jane Gwiazda Ph.D, FARVO, FAAO
Director of Graduate Studies

New England College of Optometry

MECHANISMS OF MOTION SHARPENING IN STEREOSCOPIC MOTION IN DEPTH

Jeff Ferrucci
New England College of Optometry, 2018

Purpose: Motion sharpening renders moving blurred images perceptually sharper than when stationary. The purpose of this study is to isolate and analyze the additional sharpening effect observed in stereoscopic motion in depth versus simple lateral motion. We have examined whether asymmetric motion sharpening, a retinal process that sharpens only the trailing edges of moving ocular images, caused the difference between stereoscopic and lateral motion sharpening. This was accomplished through three experiments. Exp. 1 verified the presence of asymmetric motion sharpening in our blurred motion stimuli. Asymmetric sharpening was removed from blurred moving images in Exp. 2, allowing for the isolation and measurement of stereoscopic sharpening associated with symmetrically blurred ocular images. Finally, Exp. 3 demonstrates the effect of combined symmetric and asymmetric sharpening on stereoscopic and lateral motion sharpening.

Methods: 10 normally binocular young adults viewed digital images on a 3D display at a distance of 106.9 cm. The images were two 1°w x 2°h bars of 14.5 cd/m^2 luminance and 50% contrast on a dark gray background. In Exp. 1, monocular test bars appeared for 0.5 sec above or below a fixation cross at random. The leading edge blur of a test bar was matched to the constant 42' trailing edge blur by a PEST staircase technique for all combinations of eye, lateral motion direction, and velocity (0.5 or 2.0Δ/sec). In Exp. 2, the relative disparity of the test stimulus changed linearly at velocities of 1.0 or 4.0°/s sec to generate the effect of motion in depth. The match values obtained in Exp. 1 were applied to the ocular test images. The stereoscopic test and static comparison images appeared simultaneously for 0.5 sec,

above and below a fixation cross. The static comparison image blur was adjusted by a PEST adaptive staircase to match the moving image perceived blur. In control trials, the bars were presented in a similar manner except that the moving test image moved laterally rather than in depth. All conditions were repeated 3 times by each subject. In Exp. 3, all parameters for measuring perceived blur in stereoscopic motion-in-depth were maintained from Exp. 2, except for the process of perceptually matching leading and trailing edges.

Results: In Exp. 1, the presence of asymmetric motion sharpening of trailing edges was verified and found to be significant. The leading edge blurs had to be reduced by 19.6% at 2°/s to match trailing edge blurs ($F=92.5$, $p \leq 0.0001$). The effect of target velocity on sharpening was highly significant ($F=92.5$, $p \leq 0.0001$) although the magnitude of sharpening differed between subjects ($F=3.13$, $p = 0.0028$). In Exp. 2, motion sharpening was significantly greater in stereoscopic motion in depth than in conjugate lateral motion at 2°/s ($F=6.68$, $p=0.036$). The overall effect of velocity was highly significant for both lateral and depth trials ($F=197$, $p \leq .0001$). The motion sharpening differed between subjects ($F=31.9$, $p \leq .0001$). In Exp. 3, stereoscopic motion sharpening was again stronger than lateral motion sharpening at 2°/s ($F=7.11$, $p=0.032$). The stereoscopic motion-in-depth sharpening was not different between Exp 2 and 3 ($F=1.2$, $p=0.37$) suggesting that sharpening by the symmetric and asymmetric mechanisms is non-additive.

Conclusions: Asymmetric motion sharpening occurs for stimuli of the type used in this experiment. When asymmetric motion sharpening is neutralized, stereoscopic sharpening is still stronger than lateral motion sharpening. The relative strength of stereoscopic motion sharpening is not significantly increased in the presence of both sharpening mechanisms.

ACKNOWLEDGEMENTS

I would like to thank my research advisor, Dr. Glen McCormack, for his unwavering enthusiasm in every element of the study. I am grateful to have worked with such an expert in the field of binocular vision. I would also like to thank my committee members, Dr. Peter Bex, Dr. Rucker, and Dr. Thorn. Special thanks to Alexandra Curran for her ceaseless support and motivation throughout every step of the process.

TABLE OF CONTENTS

CHAPTER 1: INTRODUCTION

1.1 The Relevance of 3D Vision……1

1.2 Cues for Depth……2

1.3 Generating 3D Images……..……..……..……..6

1.4 The Mechanism of Simulated Depth Perception…….……...…….8

1.5 Theories of Visual Discomfort…….…….……10

1.6 The Study of Perceived Blur in Moving Images…….……..……12

1.7 The Perception of Blur with Stereoscopic Images…….15

1.8 Stereoscopic Sharpening: Statement of the Problem…….17

CHAPTER 2: GENERAL METHODS

2.1 Subject Selection……...….20

2.2 Subject Scheduling…….…….…….…….……...……..21

2.3 Informed Consent…….…….…….……...…….22

2.4 Lab Equipment and Setup…….…….…….……..…….22

CHAPTER 3: EXPERIMENT ONE: MONOCULAR EDGE MATCHING

3.1 The Purpose of Monocular Edge Matching…….…..24

3.2 Procedures for Monocular Edge Matching……..…..24

3.3 Analysis of Monocular Edge Matching Data……...…..25

3.4 Results Monocular Edge Matching……..…..26

CHAPTER 4: EXPERIMENT TWO: EDGE MATCHED STEREO-SHARPENING

4.1 The Purpose of Evaluating Edge Matched Stereo-Sharpening……..28

4.2 Procedure for Edge Matched Stereo-Sharpening……..28

4.3 Analysis of Edge Matched Stereo-Sharpening Data…….30

4.4 Evidence for Edge Matched Stereo-Sharpening Data……...30

CHAPTER 5: EXPERIMENT THREE: EDGE UNMATCHED STEREO-SHARPENING

5.1 The Purpose of Evaluating Edge Unmatched Stereo-Sharpening……32

5.2 Procedure for Edge Unmatched Stereo-Sharpening ……32

5.3 Analysis of Edge Umnatched Stereo-Sharpening Data……32

5.4 Evidence for Edge Unmatched Stereo-Sharpening Data……..…33

CHAPTER 6: GENERAL DISCUSSION

6.1 Implications of Stereo Sharpening……....35

6.2 Complications and Limitations of the Study…….....41

6.3 Applications for Future Research…….….42

CHAPTER 7: APPENDIX

7.1 Purpose of the Pilot Experiment……45

7.2 Procedure for the Pilot Experiment……...….46

7.3 Analysis of the Pilot Study Data……...….47

LITERATURE CITED……...…….49

LIST OF FIGURES AND TABLES

Figure 1: Paleolithic cave drawing of the Grotte Chauvet-Pont d'Arc……..3

Figure 2: Masaccio, *The Tribute Money*……4

Figure 3: Pixar, *The Blue Umbrella*……...5

Figure 4: *The Wheatstone Arch,* Sir Charles Wheatstone……..….6

Figure 5: Hanna-Barbera, *Tom and Jerry*……...……12

Figure 6: Match blur vs Retinal Image Velocity, McCormack et al, ARVO 2013……17

Figure 7: Bedell's hypothesis, Stereo vs Conjugate lateral Images…….18

Figure 8: Calibrated Screen Luminance……...…..23

Figure 9: Blur Range……...23

Figure 10: Experiment 1 stimuli……..25

Figure 11: Experiment 1: Trailing Edge Sharpening Results……..27

Figure 12: Experiment 2: Conjugate Lateral Stimulus……..……..29

Figure 13: Experiment 2: Stereo Near Motion Trial Stimulus……....29

Figure 14: Experiment 2: Edge-Matched Stereo Sharpening Results……...…..31

Figure 15: Experiment 3: Edge-Matched Stereo Sharpening Results…….34

Table 1: Subject Screening Results……..44

Figure 16: Examples of Logistic and Weibull Curves……...…..47

CHAPTER 1

INTRODUCTION

1.1 The Relevance of 3D Vision

Increasingly, mainstream media popularizes the use of three dimensional displays. The technology has become widely available over the past decades, first debuting in the Victorian era in the form of Wheatstone Stereoscopes (Howarth, 2011). The technology advanced in the 1950's with the earliest models of stereoscopic televisions. Today, feature films offer 3D adaptations of nearly every new cinematic release. The consumer can even utilize the technology in their own home with televisions and devices such as the Nintendo 3DS and NVIDIA GeForce active flicker compatible PC monitors. Not surprisingly, the three dimensional content is popular with young children who may view the displays for hours at a time.

The technology also has applications in the medical field. Ophthalmic imaging, mammography, vascular imaging, and medical training all utilize stereoscopic displays (Held and Hui, 2011). Fine details in anatomy such as the cupping of an optic nerve or spatial relationships between levels of vasculature on the retina are best appreciated with stereopsis. The clinical benefits of stereopsis are obvious for an assessment of the fundus of the eye when comparing binocular views versus monocular direct ophthalmoscopes or fundus photography assessment. 3D displays give clinicians the advantage of documenting findings for later review with stereoscopic fundus photography.

Although the technology appears to be well received by the public, some report discomfort with symptoms such as asthenopia, diplopia, headaches, and motion sickness (Shibata, Kim, Hoffman, and Banks, 2011), (Hoffman, Girshick, Akeley, and Banks, 2008) (Aznar-Casanova, Romeo, Gomez, and Enrile, 2017). The prevalence of stereoscopic entertainment raised concerns in the 1980s. The cause of this discomfort was not well understood. Governments began to require disclaimers on 3D products. In fact, the Italian government seized thousands of the earliest 3D glasses which failed to disclaim a risk of generalized vision problems (Howarth, 2011). A theory for the visual symptoms with prolonged 3D viewing emerged around this time, addressing similar concerns with head mounted displays. This theory involves accommodation-convergence mismatch, still regarded by many researchers as the likely cause of visual discomfort with stereoscopic displays.

1.2 Cues for Depth

Long before the invention of stereoscopic displays and devices artists sought to depict depth in their artwork. Artists like Brunelleschi, Rafael, and Da Vinci may have mastered perspective in the Renaissance, however even early Paleolithic cave drawings dating back to 30,000 BC engage with depth perception. The paintings of the Chauvet-Pont-d'Arc Cave are the earliest examples of monocular depth cues (Brooks, 2017). These cues are able to convey depth through simple techniques such as occlusion, shadowing, and familiar size (Held et al, 2011). In the earliest cave drawings, the forms of animals in the foreground occlude imagery

more posterior in depth. Similarly, foreground images can cast shadows on posterior objects to establish the depth of a scene.



Figure (1): Paleolithic cave drawing of the Grotte Chauvet-Pont d'Arc

These techniques were further perfected throughout the 14th and 15th century. Brunelleschi, a master of architecture and perhaps most well known for designing the Duomo on the Florence Cathedral, demonstrated the earliest form of linear perspective in his sketch of the Florence Baptistry (Brooks, 2017). In the works of Masaccio a vanishing point exists as a far point in the image, as seen in *The Tribute Money*. Converging lines towards the vanishing point create a diminishing relative size of objects, moving posteriorly from the foreground imagery (Held et al, 2011). Familiar size is a powerful monocular depth cue. In the image below, the mountain backdrop establishes a far point in the background due to their relative size compared with the men in the foreground.



Figure (2): Masaccio, *The Tribute Money*

Many consider Caravaggio "The Master of Light" for his use of shadow to create captivating compositions with convincing depth. Artists who were heavily influenced by his works were referred to as "The Shadowists." Shadowing, often in combination with occlusion enhances the depth of an image (Held et al., 2011). The use of light and occlusion provide information on the relative positions of objects. Well lit forms most often appear in the foreground with shadowed and occluded images looming in the background. Nearly every convincing depiction of real world settings combine these elements, mimicking the monocular cues of our world. Interestingly, the depiction of focus and blur is often absent from these famous works. Photography and digital art, such as the animations from Disney, Pixar, and Dreamworks include physical image blur associated with the real world phenomenon of focal points. In the image below, from Pixar's *The Blue Umbrella,* depth is depicted with the use image blur in addition to shadowing and occlusion. A mid-ground is established by blurred objects both in the foreground and background. In a study of image

blur in naturalistic settings, Taylor and Bex report that viewers are able to appreciate a range of blur levels in a scene. In their study, viewers were able to discriminate between up to four discrete blur values for the stimuli tested. Taylor and Bex argue that when utilized in combination with other monocular depth cues, image blur can enhance the perception of depth in 2D images (Taylor and Bex, 2015).



Figure (3): Pixar, *The Blue Umbrella*

Despite the use of monocular cues, a flatness of these images still persists. Viewers do not experience the same illusion of 3D depth obtained from binocularity and stereopsis. Experimenting with the limitations of depth in artwork, Leonardo Da Vinci and Jacopo Chimenti created the first stereoscopic images long before the Wheatstone and Brewster stereoscopes of the Victorian Era (Brooks, 2017). Images drawn with discrete differences of perspective, can be presented monocularly, simultaneously to either eye creating a compelling sense of depth.

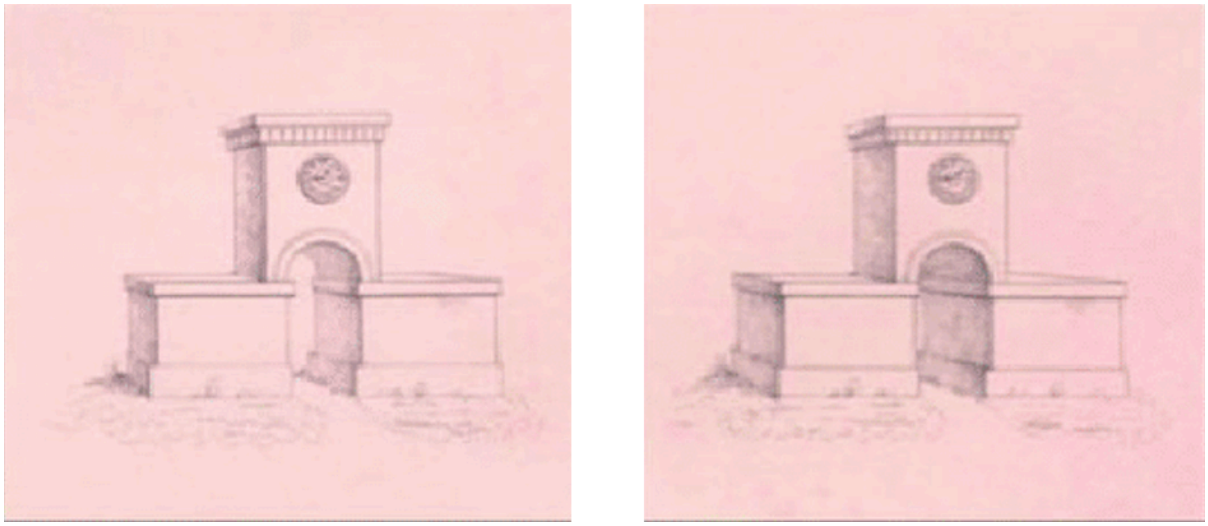


Figure (4): *The Wheatstone Arch,* Sir Charles Wheatstone

As with images in the device, there is a small disparity between images viewed in real world settings due to the offset in positioning of the human eye. The pupillary distance between the two eyes provides a slight difference in perspective, creating image disparity necessary for stereopsis. Depth and perception enabled by binocular vision provides a distinct advantage over depth perception from monocular cues alone.

1.3 Generating 3D Images

The design of 3D imagery has not changed significantly since the origin of the Wheatstone and Brewster stereoscopes (Kollin and Hollander, 2007). Advancements in the technology used to view these images, however, has allowed for different applications. 3D images are simply composed of two similar images that can be fused when presented monocularly to either eye. Binocular disparity, the differences between the images, simulates stereopsis. Colored filters, polarizing filters, and active shutter glasses such as

those most common with 3D televisions and PC monitors today can be used to present the similar images to either eye.

Colored filters are an inexpensive and popular way to dissociate an image during binocular viewing. The two similar images composing a 3D image are rendered in separate colors. The image meant for the left eye can be colored red, whereas the image meant for the right eye can be colored green. A red-free lens over the right eye and a green-free lens over the left eye will only transmit a portion of the superimposed images, allowing for the computation of disparity by the binocular system (Howarth, 2011).

Similarly, polarizing filters are able generate depth from images. These glasses utilize polarizing lenses which transmit inverse phases of polarity to either eye. This once again allows for the computation of disparity of the two similar images by the visual system. This method is most commonly used in cinema. Many viewers are able to view the same source image, each experiencing the intended depth effect (Howarth 2011).

Active shutter glasses are a more expensive solution, more commonly used with televisions and PC displays. Unlike polarizing filters, which sacrifice the luminance of an image, active shutter glasses are able to present the full picture alternately to either eye at a frequency of 120Hz. This process is rapid enough for a seamless integration of the images and binocular comparison can occur for the perception of depth (Howarth 2011).

1.4 The Mechanism of Simulated Depth Perception

Humans demonstrate binocularity early in life, developing fusion and stereopsis by 3 months of age (Fawcett, Wang, and Birch, 2005). Stereopsis continue to rapidly improve in the succeeding months until 18 months of age, with gradual improvement continuing into the first three years (Fawcett et al., 2005). This critical period for the development of stereopsis is sensitive to disruption in the form of monocular disruption or eye misalignment (Fawcett et al., 2005). Children with a history of amblyopia or strabismus fail to discern small discrepancies between the ocular images (retinal disparity) and have poor stereopsis as a result (Aznar-Casanova et al., 2017).

Our visual system evaluates retinal disparities constantly throughout everyday life. The small amount of disparity between our two eyes allow us to complete near tasks more efficiently with stereosopic depth perception. There are, however, inherent differences between perceiving depth in the natural world and viewing images with simulated depth on 3D displays. Cross talk, accommodation-convergence mismatch, and the absence of motion parallax are examples of the many obstacles to a convincing simulation of depth (Howarth, 2011). Red-green filters are a simple mechanism for generating stereo images on digital displays that suffers from "cross talk" artifacts. Partial transmission of images due to imperfectly matched stimuli can create a bleed through effect, interfering with the intended monocular presentation of the image components. Red-green filters also limit the use of color in the images (Howarth, 2011).

Active flicker glasses overcome the limitations of color and significantly limit the amount of cross talk between the two eyes, however, still suffer from an absence of motion

parallax in which the viewer's head movements are not accurately translated into the perception of the scene. In a real world setting, a viewer gains information on depth through lateral head motion, gaining additional information about the relative location of objects through motion parallax which is not possible when viewing a 3D display (Howarth, 2011).

Most publications agree that these inherent differences between displays and real world viewing are multifaceted with visually induced motion sickness and accommodation-convergence mismatch in the forefront of the discussion. Visual induced motion sickness (VIMS) results from a discrepancy between the visual perception of motion and the absence of true movement (Howarth 2011). The effect is analogous to visual-vestibular mismatch, which causes seasickness, when an individual views a stable setting but experiences vestibular motion.

Accommodation convergence mismatch is a phenomenon unique to visual displays. This problem is due to a discrepancy within the visual system. The retinal disparity generated by 3D displays triggers the vergence mechanism, which in turn stimulates the accommodative system. In a real world setting this is appropriate. In the case of a 3D display, the induced accommodation causes image blur. The aberrant blur is corrected when the viewer accommodates back to the plane of the display causing a mismatch in the typical correlation of vergence and accommodation (Shibata et al., 2011).

1.5 Theories of Visual Discomfort in 3D Displays

Many viewers report eye strain and fatigue with stereoscopic and head mounted displays (Hoffman et al., 2008), (Shibata et al., 2011). Although a considerable amount of research has been done to find the culprit of these symptoms, results have been highly variable on the impact of mechanisms involving the oculomotor and accommodative systems.

Many publications agree that accommodation-convergence mismatch as the likely culprit (Turnbull and Phillips, 2017), (Hoffman et al., 2008), (Shibata et al., 2011). Hoffman et al. quantified discomfort symptoms and visual performance deficits caused by mismatch of vergence and accommodation (Hoffman et al., 2008). Hoffman et al. argue that the conflicts between accommodation and vergence affect binocular fusion and cause visual fatigue. In this study, a specialized apparatus was used to directly measure the correlation of accommodation, vergence, stereoacuity, and discomfort. When the natural relationship between accommodation and vergence is maintained, the time necessary for fusion was reduced, stereoacuity was increased, and perception of depth distance is more accurate. Furthermore, viewers reported visual fatigue and discomfort with a mismatch between accommodative and vergence (Hoffman et al., 2008).

Shibata et al. expands upon Hoffman's study of accommodative-vergence mismatch by analyzing the effects of focal distance versus vergence distance. The plot of this relationship is commonly known as the "zone of clear and single binocular vision" (ZCSBV), first interpreted by Donders in 1864 (Shibata et al., 2011). Percival continued to interpret the relationship, suggesting that viewers were most comfortable with stimuli with a relationship

between focal and vergence distance which lies within the inner third of the ZCSBV. Similarly, Sheard claimed that the zone of comfort lies within the ZCSBV, but extended instead from the plot of the phoria line to one third of the distance toward the maximum and minimum relative vergence lines bounding the ZCSBV (Shibata et al., 2011).

Shibata et al. utilize the ZCSBV to analyze an individual's phoria and the probability of discomfort with accommodation-vergence conflicts at varying focal distances. Discomfort was quantified with a questionnaire polling visual clarity and fatigue as well as neck, back, head, and eye irritation. A significant difference in clarity, eye fatigue, and eye strain was noted for conditions with accommodative-convergence mismatch. No significant difference was noted with a change in focal distance, although viewers tended to report worse symptoms with near distances. Their analysis of the ZCSBV data shows that subjects reported greater discomfort with uncrossed disparity (divergent) conditions and at large focal distances, the difference in symptoms for matching accommodation-convergence cues versus mismatched cues was less significant.

While these studies suggest mechanisms for discomfort, it is still not obvious why a mismatch between the accommodation and convergence systems causes discomfort. We wondered whether discomfort caused by accommodation/convergence mismatch was more correlated with objective ocular image defocus, or the subjective impression caused by ocular image defocus.

1.6 The Study of Perceived Blur in Moving Images

Moving images undergo both sharpening and smearing processes. These effects appear to depend on the spatial frequency of images, with deblurring mechanisms operating more efficiently on images with lower spatial frequencies and motion smear occurring for images of higher spatial frequencies. Hammett et al. report that motion sharpening processes appear to occur for objects physically blurred by a value greater than 10 minutes of arc, whereas objects blurred less than 10 min arc underwent motion smearing (Hammett, Georgeson, and Gorea, 1997).

It is likely that the layman would predict that fast moving objects are associated with a motion blurring of the trailing edge, perhaps in the form of smearing as depicted in many animations and cartoons. It is common practice that objects in motion are drawn with a lengthening or smearing of form.



Figure (5): Hanna-Barbera, *Tom and Jerry*

These conventions are influenced by observations made in the natural world. Leonarda Da Vinci commented on the appearance of a tail with luminous objects in motion (MacCurdy, 1956). Newton made similar remarks for the basis of image persistence (Newton, 1730). The human visual system integrates forms of moving objects over a duration of 35ms (Hammett et al, 1997) (Gorea and Tyler, 1986), (Georgeson, 1987) to a maximum of 120ms (Barlow, 1958), (Legge, 1978). The integration of stimuli drifting throughout this period of time should in theory be perceived as blurry or smeared. The multiple states of a stimulus throughout the integration period will be perceived as a single smeared form by the visual system (Chen, Bedell, Ogmen, 1995), (Paakkonen and Morgan, 1994), (Hammet et al, 1997). A quickly moving dot image for example, may appear to have a tail due to a drift in location during the integration period. The amount of perceived motion blur is dependent upon the length of integration, with shorter times limiting the amount of blur perceived. (Burr D, 1980). A study by Burr et al. on motion smear, however, found a less than expected amount of blur based upon their understanding of integration time alone.

Tourancheau et al. observed a similar effect while verifying the presence of motion blur artifacts with LCD monitors. The liquid crystal display is a popular design adopted by many consumer electronics including televisions, PC monitors, and cell phones. The inherent sample-and-hold technique of the displays is responsible for a persistence of images. The perception of motion blur created by persisting images was, however, less than the physical measures of LCD monitor motion blur by the Moving Picture Response Time measure utilized in the study. They report that the mechanism responsible for the difference

in physical versus perceived measures of motion smear is due to a well reported motion sharpening phenomenon (Tourancheau, Le Callet, Brunnstrom, Andren, 2009).

In a study of illusory distortion of moving form by motion deblurring, Marinovic and Arnold found that the trailing edges of images are flattened for disks following a circular path. They suggest that this evidence for motion sharpening is due to a retinal masking process initiated by the image's leading edge 60ms before the trailing edge occupies the same visual space. (Marinovic and Arnold, 2013)

Revisiting motion deblurring in human vision, Burr and Morgan evidenced a few additional details for motion sharpening. The just noticeable difference for discriminating between degree of blur increases with the amount of baseline blur. This indicates that it is tougher to discriminate between similarly blurry images when the physical degree of blur is large. The effects of motion blur may simply be lost due to the limitations of blur sensitivity for stimuli of that type. They further argue that the presence of motion sharpening effects is simply due to an inability to discriminate degrees of blur with objects in motion (Burr and Morgan, 1997).

Bex et al. support the idea of a motion sharpening mechanism over the inadvertent deblurring process proposed by Burr et Morgan. Blurred sinusoidal gratings in motion appear sharper than blurred gratings. The perceived sharpness of the image is greater than its physical blur value. This indicates the addition of motion sharpening onto images rather than a limitation of motion blur as suggested by Burr and Sylvain. In other words, the expected motion smear was not just limited for objects in motion, rather the perceived blur was reduced compared with the physical blur of the image. (Bex, Edgar, and Smith, 1995).

Bex et al., further analyze motion sharpening in relation to stimulus contrast. In a preceding study, Burr and Ross provide evidence for a relationship between image motion and contrast perception (Burr and Ross, 1982). Bex et al., demonstrate a significant effect of contrast on blur perception, noting that higher contrast images appear sharper than low contrast images moving at similar speeds (7.2 degrees/second). Bex et al., comment that although the contrast does have an effect on blur perception with images in motion, this relationship alone cannot fully explain motion sharpening considering the findings of Thompson. Thompson evidences an inverse relationship between contrast and image velocity at high temporal velocities. (Thompson, 1982).

Hammett et al. similarly evidence support for the relationship between contrast, image speed, and blur perception. Additionally, they claim that the physical blur of the image is the more essential factor in motion sharpening. While contrast and image speed demonstrate a significant relationship with motion sharpening, the effects are much greater when subjects view blurrier images. Hammett et al. report that images physically blurred by greater than 10 min arc consistently underwent sharpening processes whereas sharper images were subjected to motion smear regardless of image velocity (Hammet et al 1997).

1.7 The Perception of Blur with Stereoscopic Images

McCormack et al. investigated the range of convergence and divergence that allow clear and single vision when watching images move in depth on a 3D display (Hogan, McCormack, and Tseng, 2012). With a stimulus to convergence, the accommodative system is invoked as well, causing aberrant focus. This optical blur however is not perceived as

expected by viewers of 3D displays. Instead, there is an apparent sharpening of the image. There must be non-optical mechanisms that clear the image, that is, motion sharpening. Multiple publications have sought to explain the mechanism of motion sharpening. Andersen and Van Essen propose a cortical shifter circuit which control inhibitory, sharpening processes for stimuli with certain retinal velocities (Anderson and Van Essen, 1987). Burr, Ross, and Morrone propose that the effect of motion sharpening may be due to the summation of retinal images falling on temporally oriented receptors (Burr, Ross, and Morrone, 1986).

Perhaps explanations for motion sharpening lie in additional neural processes. There are potentially, multiple mechanisms that contribute to the perception of motion sharpening. McCormack's previous experiment, in collaboration with Mr. Joe Van Cura and Dr. Peter Bex, provides insight into how our visual system sees image blur in a 3D setting (McCormack et al., 2014). It appears that an image is perceptually sharpened by the visual system for laterally moving images and even more so with motion in depth. McCormack et al. proposed that the sharpening associated with stereoscopic motion in depth was caused by enhanced contrast and sharpening behaviors in cortical stereoscopic motion neurons compared to conjugate motion neurons. The results were presented at ARVO in 2013.

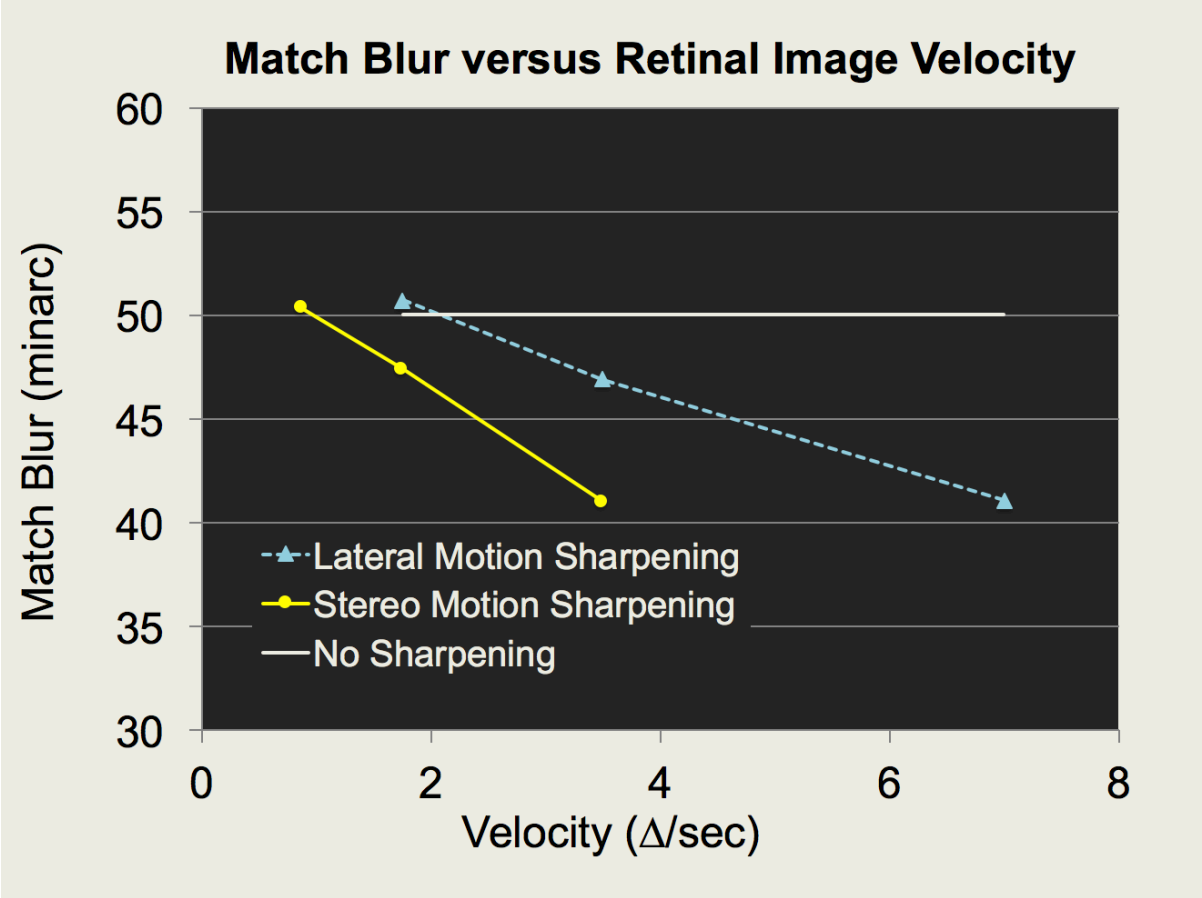


Figure (6). A graphic representation of the findings presented by McCormack et al at ARVO 2013. Blurry moving images are perceptually matched to a static comparison image with a known amount of blur. Lower match blur values indicate sharper images. McCormack's data suggests that the phenomenon is stronger in the 3D images. Note that for the 3D image, the match blur value is significantly lower than in cases of lateral motion. This indicated that the effect of stereo motion sharpening is greater than for lateral sharpening (McCormack et al, 2014).

1.8 Stereoscopic Sharpening: Statement of the Problem

At the 2014 annual meeting of The Association for Research in Vision and Ophthalmology Dr. Harold Bedell commented that McCormack et al's results are possibly confounded by the fact that the motion sharpening perception may be symmetric, that is, the

trailing edges of moving blurred bars may be sharpened more than the leading edges. For instance, in a right moving, physically symmetric, blurred image, the perception may be that the left, trailing edge is sharper while in near motion the temporal edges appear sharper (see Figure 7).

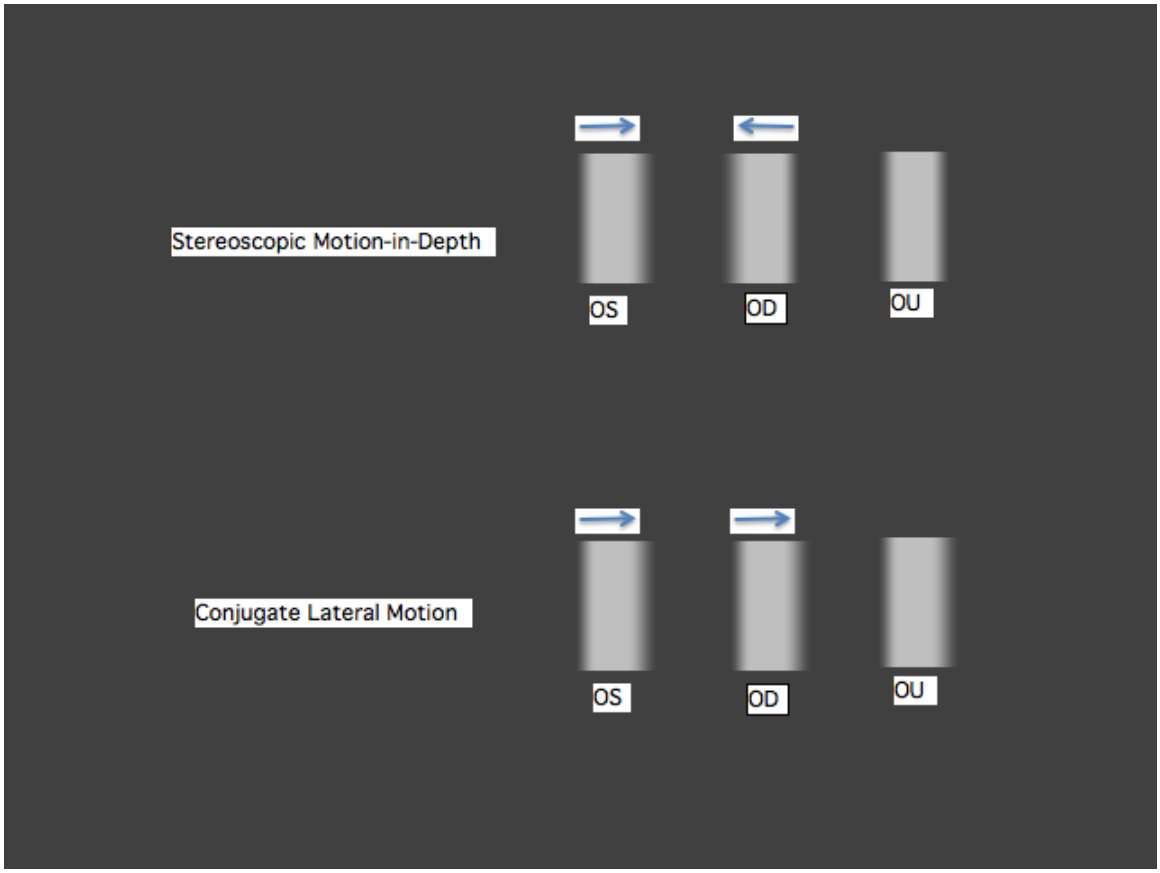


Fig. (7). Bedell's hypothesis: In stereoscopic motion-in-depth (above) the right and left eyes' ocular images (OS and OD) are moving nasally in the visual fields (direction of arrows) during near motion. The trailing temporal edges are sharpened more than the leading nasal edges. In binocularity (OU) the sharpened temporal edges fuse with the more blurred nasal edges, but the more sharpened ocular half-image of each fused edge dominates edge perception. One would expect both fused bar edges to be as sharp as the sharper trailing edge of each eye's image. During conjugate lateral motion (below), the ocular images are both moving rightward, with the trailing left edges being sharpened more than the leading right edges. The fused image (OU) is expected to look like the monocular images (OS and OD), with less overall sharpness than in the binocular stereoscopic image.

If this phenomenon is shown to be significant, McCormack's previous claim that motion in depth produces stronger motion sharpening effects than lateral motion is called into question. With motion in depth, there are essentially two oppositely moving bars presented to the eyes. It is possible that stronger stereoscopic motion sharpening is due to an additive effect of monocular blur asymmetries, and not to special properties of stereoscopic motor neurons. Sharp, defined detail tends to dominate human perception. If a subject were to fuse two blurred images, one with a sharper left edge and the other with a sharper right edge, the perception may be an overall sharp bar when blur information is discarded by neural interpretation of the stimuli. Therefore, it is possible that the stronger motion sharpening in stereoscopic motion in depth may have been due solely to asymmetric monocular sharpening in each eye's image.

The purpose of my experiment is to first address whether or not blur asymmetry exists in laterally moving blurry bar stimuli of the type used by McCormack et al., and then observe whether additional motion sharpening with stereoscopic motion in depth is still present when perceived edge blur asymmetry is removed from the moving monocular images that compose stereo motion. If both asymmetric and symmetric motion sharpening are verified, we will investigate the additivity of these two mechanisms.

CHAPTER 2

GENERAL METHODS

2.1 Subject Selection

Subjects were screened for clinically normal binocular vision and excluded from the study if they did not qualify. These standards included normal ocular and general health by subject report, normal Borish Card 40cm stereoscopic acuity (threshold <= 30"), 20/20 corrected visual acuity in each eye, far phoria by alternating cover test within 2 eso to 3 exo, near phoria by alternating cover test within 8 exo to 2 eso, normal near-point of convergence (within 6cm from nose), and normal amplitude of accommodation for age determined by Hofstetter's formula for minimum normal. All subjects were screened at the New England College of Optometry using equipment in the clinical practice rooms. Subjects were screened by Jeff Ferrucci or Dr. Glen McCormack. The same equipment and standards were used for each subject.

Experiment 1 will determine if our subjects are good candidates for psychophysical experiments. Data with excessive noise and data suspicious for changing blur criterion, in which the subject appears to have applied a bias or strategy in the middle of testing, will not be considered appropriate for Experiment 2 and Experiment 3 due to the potential for unreliable threshold calculations. No subjects were, however, rejected due to their results in Experiment 1. The same subjects will participate in all experiments, however, not all subjects will need to complete the third Experiment.

12 subjects were screened for eligibility, 10 of which fit standards of normal binocularlity and were enrolled. The two subjects that failed the screening process

demonstated phorias outside of the acceptable range (5 eso at near and 9 exo at near). Of the 10 candidates, one subject did not return for the final experiment and was not analyzed in the results of this study. Ultimately, 4 male and 5 female young adults aged 18-35 years completed the study for a total population of 9 subjects. (Please refer to the appendix for further information on the enrolled subjects). Five of these enrolled subjects first participated in a pilot study to determine the most appropriate adaptive staircase technique used throughout the three experiments (Please refer to the appendix for further information on the pilot study).

2.2 Subject Scheduling

Subjects were able to complete the experiment in three sessions which ran approximately 1.5 – 2 hour each. Session 1 included the screening procedures and three repeats of Experiment 1 if the subject was found to be a suitable for the study. After an analysis of the Experiment 1 results, the subjects were asked to return for three repeats of Experiment 2 and Experiment 3 on two separate days to avoid fatigue. The subjects performed the two final experiments in a random order to avoid the effect of subjects becoming practiced observers by the end of the study. It is possible that the subject could become more proficient at psychophysical tasks over the course of the study. Randomizing the scheduling date of experiment 2 and 3 neutralized the effects of learning.

2.3 Informed Consent

Subjects were asked to sign an informed consent form before the screening process began. Jeff Ferrucci or Dr. Glen McCormack served as the witness. The forms disclosed the payment and expectations for completing the three sessions of the study.

2.4 Lab Equipment and Setup

An Asus PC (M32AD-US033S) served to generate images using Matlab and Psychtoolbox software. The PC drove an Asus 278HE 27" NVIDIA 3d-enabled display via a high end NVIDIA Quadro FX 3800 video card with NVIDIA 3D Vision 2 Wireless Glasses. The Asus display featured a 1920x1080 resolution (31.25 degrees wide; 1 minarc/pixel resolution at a viewing distance of 106.9cm), at a 120Hz frame rate. A headrest was placed at the viewing distance. Labview software running on a Mac G4 recorded subject responses, provided instructions to the Matlab for image generation, and ran the PEST psychometric adaptive staircase algorithm (See appendix for detailed information on the PEST algorithm). The Mac and PC communicated through a local TCP/IP connection.

In order to attain a screen luminance through polarized lenses that is comparable with McCormack's previous experiment (McCormack et al., 2014), a luminance meter was used to test screen luminance. Test images were generated in Adobe Photoshop to cover the entire screen gray scale from a nominal brightness value of zero to one hundred. The light meter was used to measure the physical luminance of the screen through the lenses of the Nvidia active flicker polarizing glasses (Figure 7).

The bar images were 2° tall by 1° wide, with blurry edges defined by a cosine falloff. Contrast of 50% difference for the bar images was established for the 14.5 cd/m2 mean luminance of grey background.

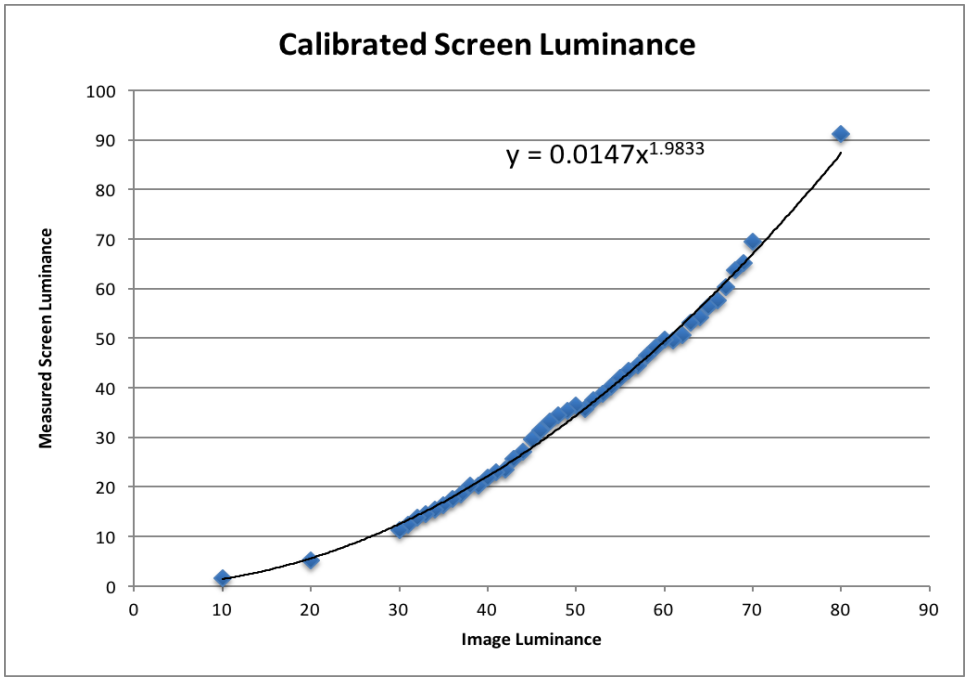


Figure (8). This graph shows the relationship between the luminance property of our digital image (x-axis) and the physical luminance of the screen when presenting that image through the polarizing lenses (y-axis). The resulting fit was an exponential that was used to generate the image blur for the experiment. It was necessary to obtain this relation to ensure the correct sinusoidal luminance that defined edge blur.

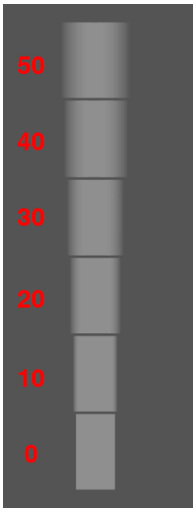


Figure (9). The bars may be presented with blur ranging from zero to sixty minutes of arc. The program can choose to present values in steps of three minutes. For example, a blur value of 42 can be compared with a blur value of 39. The luminance of the bars was calibrated by the process depicted in Figure 8.

CHAPTER 3

EXPERIMENT ONE: MONOCULAR EDGE MATCHING

3.1 The Purpose of Monocular Edge Matching

Experiment 1 verified the presence of asymmetric motion sharpening in our blurred motion stimuli. The results determined the compensatory value necessary for the leading edge to appear perceptually equal in sharpness to the asymmetrically sharpened trailing edge of the moving, blurred stimuli.

3.2 Procedures for Monocular Edge Matching

Eight different conditions were run as 8 interleaved staircases, 40 trails per staircase. Each condition was repeated three times for a total of 960 presentations to each subject. The eight conditions included all combinations of motion type (stereoscopic or lateral motion), motion direction (near/far vs. left/right), and velocity (0.5°/sec or 2.0°/sec). Note that the speed here is equal to the relative speed of the two similar images that compose a 3D stimulus and is therefore half the velocity of the binocular images of Experiment 2 and 3. The locations of the moving stimuli (above or below fixation) and the comparison image (symmetrically opposite the central fixation point) were randomized and therefore not one of the conditions assessed.

The subject will initiate each trial with the keyboard and after a 1 second delay the stimulus will move across the screen with a leading edge blur, selected by PEST, and a constant 42 degree trailing edge blur. To limit order effects on the results of Experiment 1

the stimuli are presented in a block randomized order as follows: ABBA, in which A is the dominant eye and B is the non-dominant eye.

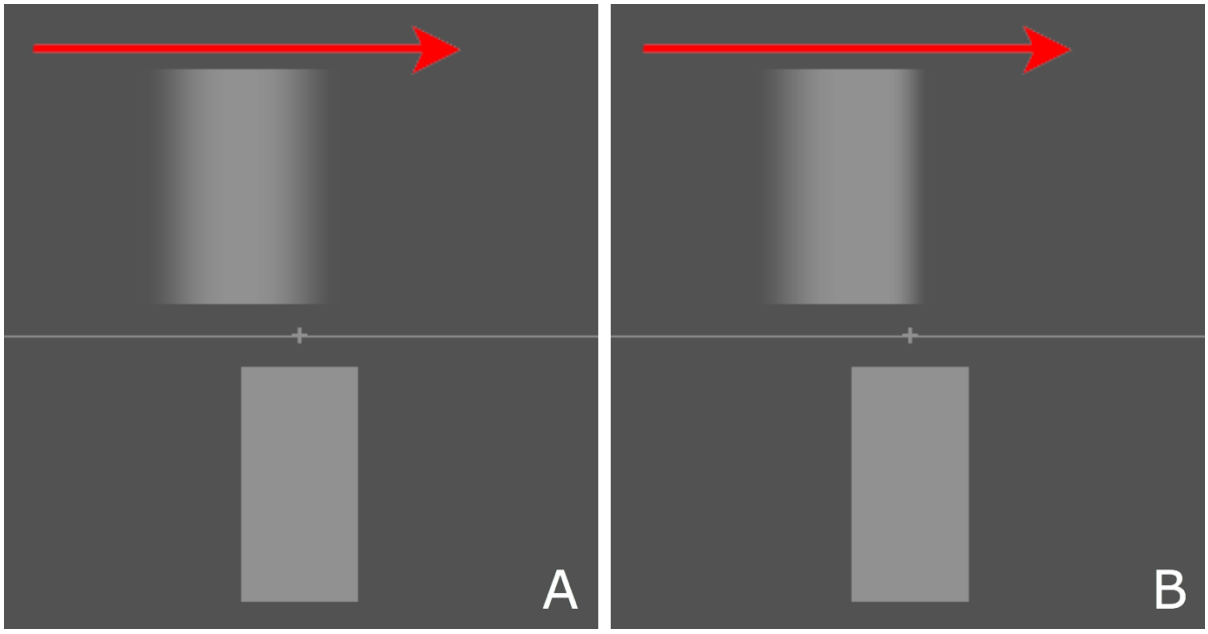


Figure (10A). Expt.1: A 60 minarc wide monocular bar is moving rightward (red arrow) with 42 minarc physically-matched leading and trailing edge blurs. The bar moves symmetrically about fixation. Figure (10B). Expt.1: The leading edge blur of the monocular bar is adjusted to match the perceived trailing edge blur by PEST. This leading edge adjustment measures monocular sharpening asymmetry. The sharp lower bar is not involved in the judgments.

3.3 Analysis of Monocular Edge Matching Data

In Experiment 1, we measured the difference of motion sharpening in the left versus right edges of bars in monocular vision. We hypothesized that monocular edge motion sharpening asymmetry exists for the test stimuli. We used Data Desk's Linear Models Repeated Measures three-way ANOVA algorithm with bar velocity as the dependent

"repeat" variable and with subject, eye, and motion direction as the independent factors. Motion sharpening will be determined as the change in match blur over velocity,

We used the velocity factor as a repeated measures dependent variable in our ANOVAs to remove much of the between-subject variability from the analysis, which is quite large. In order for true motion sharpening to be established in either experiment, it must have been proven that blur matches changed as a function of velocity, considering that all previous studies of motion sharpening have shown that sharpening depends on target velocity. In our analyses, we expected the interaction of the velocity factor with the other factors (eye, direction, subject) to be significant, demonstrating that motion sharpening had been affected by the other factors. That is, any change of sharpening due to eye, direction, or subject which did not interact with the velocity factor were deemed irrelevant to this study.

3.4 Results of Monocular Edge Matching

In the preliminary trials, the presence of asymmetric motion sharpening on the trailing edge of a laterally moving bar was verified and found to be significant. ($F=92.5$, $p\leq0.0001$). This is strong evidence that asymmetric sharpening occurs and was a potential factor in McCormack et al.'s previous study on neural sharpening with motion in depth. The 42' trailing edge controls were on average matched by leading edge blurs of 39.11' at speeds of 0.5°/sec and 33.75' at 2.0°/sec. The effect of target velocity on sharpening was highly significant ($F=92.5$, $p\leq0.0001$). The physical blur values of leading edges had to be reduced by 19.6% at 2°/s to match trailing edge blurs ($F=92.5$, $p\leq0.0001$). The physical blur values of leading edges must be perceptually matched with lower blur values, to account for the

perceptual sharpening of the trailing edges. This finding held true in all cases but for one condition in subject "BHC". In a singular condition, BHC showed a leading edge sharpening of 1.8', otherwise, BHC's results were in agreement with the rule of trailing edge sharpening. Motion sharpening asymmetry was significantly different between subject ($F=3.13$, $p = 0.0028$). BHC showed the smallest effect of asymmetric motion sharpening of all subject at a value of 2'. Subject AMC exhibited the largest effect at a value of 8'.

There was no significant relationship found between factors including the eye tested (right or left) or the direction of motion (left or right). With all subjects considered, the effect of leftward versus rightward motion was insignificant ($F=0.68$, $p=0.43$). Some subjects, however did exhibit a bias for stronger sharpening effects in a certain motion direction ($F=2.33$, $p=.017$). Overall, it is evident that motion sharpening asymmetry exists for stimuli of the type used in our experiment.

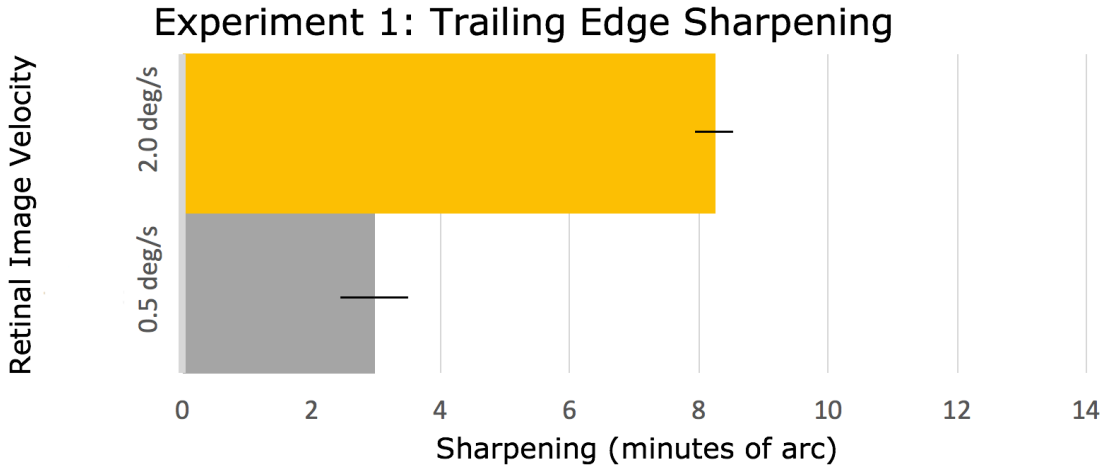


Figure (11). Amount of sharpening of the leading edge (in min. of arc) that matched the 42' blur of the trailing edge at velocities of 0.5°/sec (gray) and 2°/sec (yellow). Standard deviation is depicted with the black horizontal bars.

CHAPTER 4

EXPERIMENT TWO: EDGE MATCHED STEREO-SHARPENING

4.1 The Purpose of Evaluating Edge Matched Stereo-Sharpening

Utilizing the results of Experiment 1, asymmetric sharpening was removed from blurred moving images in Experiment 2. This allowed for the isolation and measurement of stereoscopic sharpening associated with symmetrically blurred ocular images. Binocular laterally moving and stereoscopically moving bars having the same retinal velocities test whether the bars moving laterally and in stereoscopic motion-in-depth stimulate the same motion sharpening.

4.2 Procedure for Edge Matched Stereo-Sharpening

Eight conditions were interleaved within trials of 40 different blur values. Each condition was repeated three times for a total of 960 presentations to each subject. The eight conditions included all combinations of direction (leftward, rightward, near, or far motion), and velocity (0.5°/sec or 2.0°/sec). The location of the stimuli (above or below fixation) was simply randomized. Stimulus location was not an assessed condition. The leading edges of the monocular images composing the 3D stimuli were initially set to the individual's perceptual edge match value from Experiment 1. PEST then adjusted the blur of the static comparison bar to match the blur of the moving bar. The subject initiated each trial with the keyboard as in Experiment 1. Each trial began one second after the keyboard press.

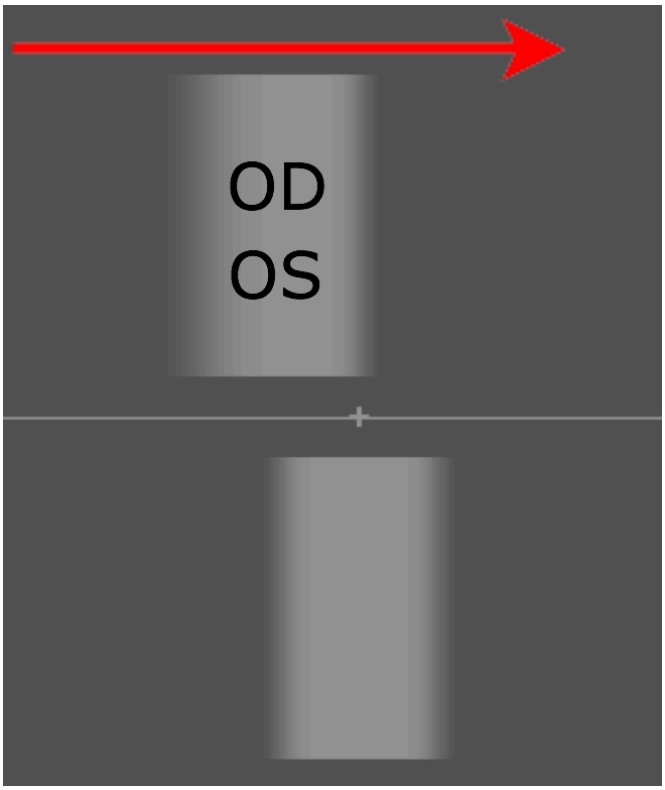


Figure (12): (Expt.2): A conjugate motion trial. Both eyes view identical edge-matched motion stimuli in which the leading (right) edges are physically sharper. The perceived blur of the moving upper bar is measured by comparison to the blur of the static lower bar.

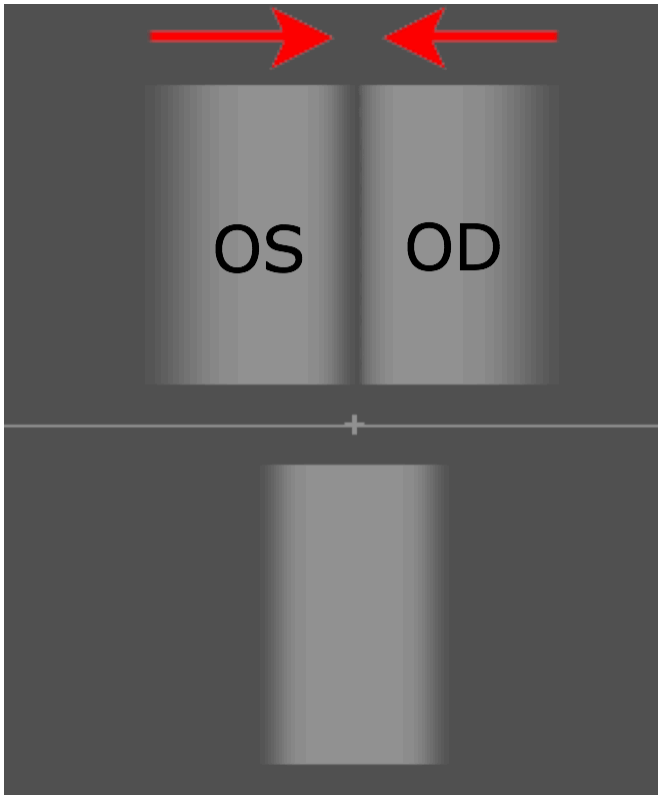


Figure (13): (Expt.2): A stereo near motion trial. The leading edges of the nasally-moving monocular images have been sharpened to match the trailing edges. The perceived blur of the stereoscopically moving fused upper bar is measured by comparison to the blur of the static lower bar.

4.3 Analysis of Edge Matched Stereo-Sharpening Data

The analysis for Experiment 2 was accomplished through a repeated measure three-way ANOVA with motion velocity (0.5°/s and 2.0°/s) as a within-subjects independent (repeat) factor and motion type (stereoscopic motion in depth versus lateral motion), motion direction (near/far in stereoscopic motion or left/right in lateral motion), and subject as between-subject independent factors. Match blur was the dependent variable. We examined the difference in match blur with a changes in velocity, binocular lateral conjugate motion versus motion in depth, and near vs far trials with stereoscopic test stimuli.

4.4 Evidence for Edge Matched Stereo-Sharpening

A mixed ANOVA evaluated the effects of motion type (lateral vs. depth), subject, and velocity (0.5°/sec or 2.0°/sec) on match blur. Motion sharpening was significantly greater in stereoscopic motion in depth than in conjugate lateral motion at 2.0°/sec ($F=6.68$, $p=.036$), revealing significant amounts of additional neural sharpening (Lateral: 40.1' at 0.5°/s, 33.4' at 2.0°/s; depth: 38.8' at 0.5°/s, 29.6' at 2.0°/s.) SE=1.99. The overall effect of velocity was highly significant for both lateral and depth trials ($F=197$, $p\leq.0001$) although the magnitude of the sharpening differed between subjects ($F=31.9$, $p\leq.0001$).

With lateral motion trials, there was no overall difference of sharpening between leftward and rightward lateral motions ($F=.0028$, $p = 0.959$); (leftward=39.9'@0.5°/s and 33.1'@2°/s; rightward=40.4'@.5°/s and 33.7'@2°/s). Some subject did exhibit an individual bias for more sharpening in certain direction, similar to findings in Experiment 1 ($F=5.31$, $p=.0004$). With motion in depth trails, there was no overall difference between near going

and far going trials (F – 0.083, p = 0.78); (near=38.9'@0.5°/s and 29.8'@2°/s; far=38.7'@.5°/s and 29.4'@2°/s) and subjects did not individually exhibit a bias for a certain direction, unlike the lateral motion trials (F=.695, p=.68).

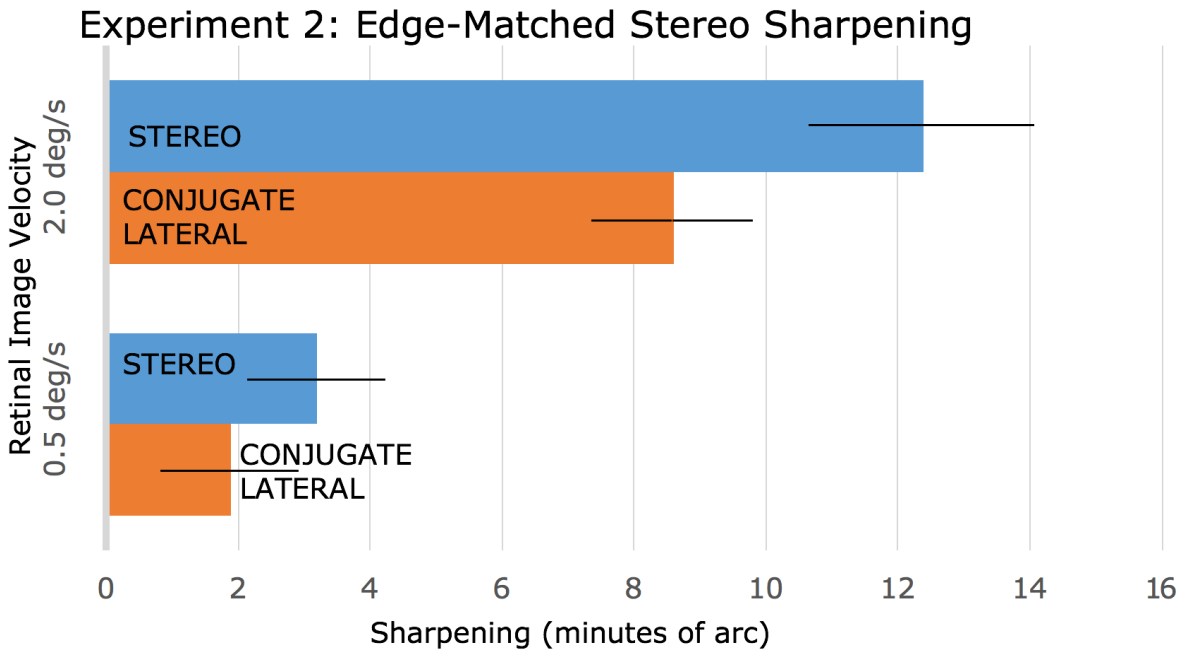


Figure (14): *Expt.2:* Amount of sharpening of the static comparison target that matched the sharpness of the stereo motion target (blue) or conjugate lateral motion target (orange) as a function of target velocities of 0.5°/sec and 2°/sec. The ocular image edges were perceptually-matched in each case. The sharpening effect appears greater with stereo motion at a velocity of 2.0 deg/sec. Standard deviation is indicated by the black horizontal bars.

CHAPTER 5

EXPERIMENT THREE: EDGE UNMATCHED STEREO SHARPENING

5.1 The Purpose of Evaluating Edge Unmatched Stereo-Sharpening

Experiment 3 served to replicate the previous study on lateral vs stereoscopic motion in depth-sharpening in Experiment 2, but without utilizing the edge-matched values determined in Experiment 1. This demonstrated the total effect of combined stereoscopic and lateral motion sharpening mechanisms.

5.2 Procedures for Edge Unmatched Stereo-Sharpening

Experiment 3 maintained all procedures from Experiment 2 except for the asymmetric sharpening compensation. The two monocular images composing the binocular test image were set with each edge physically equal, unlike the monocular images of Experiment 2.

5.3 Analysis of Edge Unmatched Stereo-Sharpening Data

The analysis of Experiment 3 was accomplished in the same manner as Experiment 2 with small variations. To discover the difference between "edge-matched" and "edge-unmatched" experiments, we collapsed each pair of match blur values from the two velocities examined, 0.5°/s and 2.0°/s, into a single differential value, slow minus fast. This differential value represented the motion sharpening magnitude. A repeated measure three-way ANOVA

compared the effect of motion type (lateral versus depth) with the matched versus unmatched process serving as the repeat factor. Motion type served as a between-subjects factor.

5.4 Evidence for Edge Unmatched Stereo-Sharpening

The overall sharpening effect was still evident in Experiment 3 ($F=20.0$, $p=.0029$) and differed significantly between subjects ($F=31.9$, $p\leq.0001$). To compare Experiment 2 and 3 more effectively, the effect of sharpening at 0.5°/s and 2.0°/s was collapsed into a single differential value. This differential value represented the motion increase in magnitude of sharpening between the two velocities. The different sharpening mechanisms appear to be non-additive by the results of the Experiment 3, considering there was no significant difference of motion sharpening compared with Experiment 2 ($F=2.8$, $p=.138$). When both mechanisms are active in Experiment 3, additional sharpening is not observed. Furthermore, there was no interaction between the motion dimension factor and the repeat factor ($F=1.2$, $p=.37$). This finding suggests that the stronger motion sharpening of stereoscopic motion over lateral motion is independent of the edge matching procedure performed in Experiment 2.

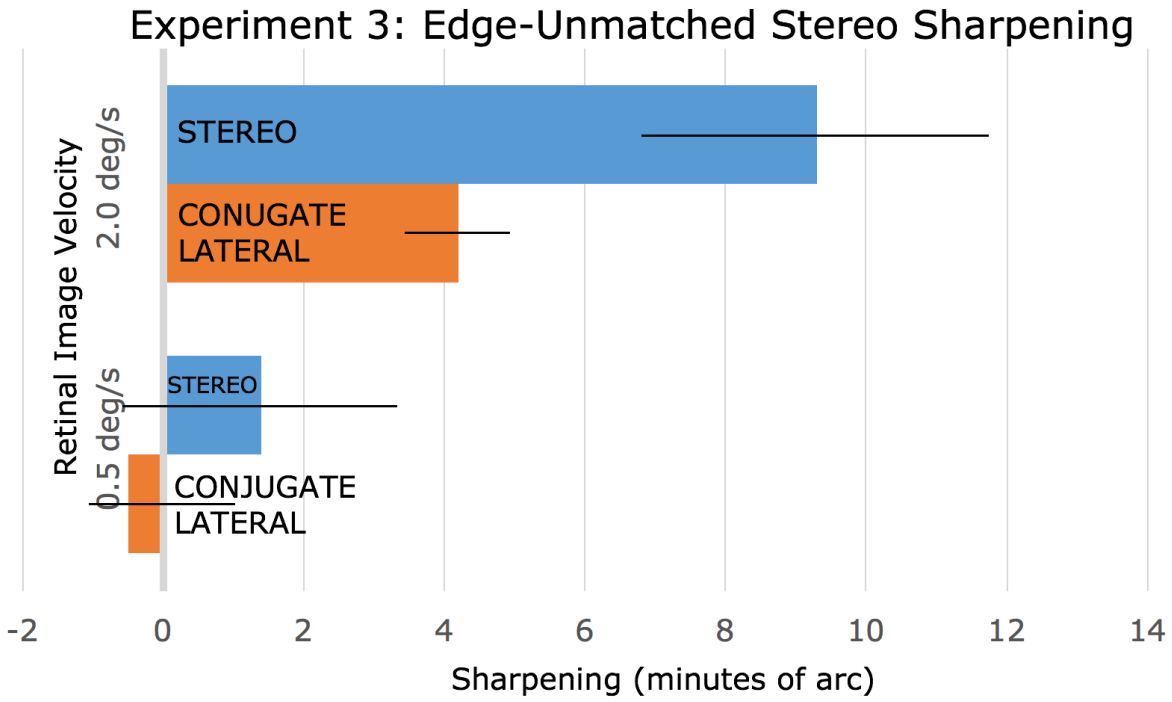


Figure (15): Expt.3. Same as Expt.2 but with the edges of the ocular images of the moving binocular target physically matched, but not perceptually matched. The sharpening effects appears greater with stereo motion at a velocity of 2.0 deg/sec. Standard deviation is indicated by the black horizontal bars.

CHAPTER 6

GENERAL DISCUSSION

6.1 Implications of Stereo Sharpening

The process of motion sharpening may at first appear counterintuitive, especially with the common perception that objects in motion appear blurry to viewers. The precept of motion blur is often utilized in film and animation to emphasize the speed of objects. This study however, evidences multiple mechanisms for motion deblurring of images in motion. Asymmetric sharpening is evidenced in Experiment 1, demonstrating a perceived sharpening of the trailing edge of blurry images. Experiment 2 and 3 demonstrate the effect of sharpening mechanisms on blurry bars with lateral, and more significantly, with stereoscopic motion in depth. The results of the experiment pose a few questions. What are the benefits of motion deblurring when the attended image is in fact truly blurry? Why are the processes of asymmetric sharpening and motion in depth sharpening not additive, leading to greater sharpening when working in combination? Most importantly, what mechanism is responsible for the greater motion sharpening noted with stereoscopic images moving in depth?

Stereopsis is a process of the visual system that allows humans to discriminate relative depth of objects for differences as fine as 1.2mm at distance of one meter. In other words, human stereoacuity can be as sensitive as 15 seconds of arc (Held et al., 2011). The process of analyzing and comparing relative disparity between objects occurs in the striate cortex. Stereopsis, however, is just one of the overwhelming number of visual processes that take place in the cortical area. It is likely that similar processes are responsible for

mechanisms of visual suppression, motion deblurring, and stereo sharpening as evidenced in this experiment.

Numerous publications have investigated mechanisms for suppressive mechanisms of blur. Many theories exist on the process with evidence for cortical suppression (Anderson et al., 1987), retinal masking (Marinovic et al., 2013), or simply poor blur sensitivity to motion blur (Burr, 1980). Burr and Morgan argue that blur discrimination is limited for image exposures longer than 150ms and shorter than 40ms (Burr et al., 1997). They do not suggest a sharpening mechanism but rather an inability for the visual system to determine the blur of a moving figure. They propose that the limitations occur due to the poor spatial sensitivity of detectors for moving images.

In this experiment we observed that asymmetric motion sharpening does in fact occur for the type of stimuli used in our experiment. Furthermore, we note the additional sharpening effect of the image with motion in depth, a process that must be independent of asymmetric motion sharpening considering its absence in Experiment 2. We propose that stereoscopic motion sharpening must be a property of cortical stereoscopic motion-in-depth cells.

This proposal coincides with the suggestion by Anderson et al., that cortical cells may be responsible for suppressive mechanisms in the form of shifter circuits (Anderson et al., 1987). The shifter circuits they describe is a hierarchy composed of cell layers with symmetrically ascending and diverging connections. Lateral inhibitory circuits may regulate the flow of information through shifter circuits leading to the suppression of pathways (Anderson et al., 1987). Anderson et al. attributes shifter circuits with the stabilization of

images on the retina in the presence of constant motion. They suggest that motion blur is suppressed through this mechanism of compensatory cortical shifts. In the realm of stereoscopic processing, suppression may come in the form of the motion sharpening observed in our experiment.

Tadin supports the cortical origin of suppressive mechanism in the form of center surround receptive fields in the primary visual cortex (V1), superior colliculus, medial superior temporal area, and medial temporal area (Tadin, 2015) (Jones, Wang, and Stillito, 2002), (Eufuku and Wurtz, 1998), (Davidson and Bender, 1991), (Allman, Miezin, and McGuinness, 1985). In studying macaque monkeys, Tadin was able to find a critical size for spatial suppression, dependent upon the eccentricity and contrast of Gabor patch stimuli (Tadin, Lappin, Gilroy, and Blake, 2003). Spatial suppression was demonstrated by the monkeys' inability to detect the direction of motion in large, high contrast stimuli. (Tadin, 2015), (Melnick, Harrison, Park, Bennetto, and Tadin, 2013). Tadin remarks that the suppressed information may not necessarily be discarded but further processed by other cortical mechanisms (Tadin, 2015).

The suppressive mechanisms demonstrated by cortical functions have potential implications in the realm of stereoscopic motion sharpening. It is possible that de-blurring processes are additional examples of suppressive mechanisms. Perhaps blur information is suppressed as cortical functions attend to the task of analyzing image motion. The additional sharpening observed with stereoscopic images may be explained by the further necessity for blur suppression in the more complicated task of tracking stereoscopic motion in depth.

Motion detection and stereopsis are just a few examples of the vast number of processes occurring throughout cortical areas of the visual pathway. Limiting the amount of information that is truly perceived is necessary in complicated, real settings. Suppressive mechanisms offer an advantage to viewers in parsing out the most salient or important components of a scene. One could argue that in our experiment, the blurry edges of the bar stimuli detract from the salience of an otherwise large, high contrast form moving across the subjects' visual field. The visual system may not require accurate blur discrimination in the task of tracking an image through space. Although the image may still appear blurry, the viewer may not be able to accurately discern the true amount of blur present. Perhaps in this way, some loss of the blur information offers an advantage in driving functions responsible for tracking the stimuli. We may consider motion sharpening as a benefit, however, perhaps it is simply an inadvertent result of lost information. One could argue that the viewer would best benefit most from an entirely accurate perception of a physically blurred image. The real benefit of motion sharpening may be that the viewer is able to more accurately track objects moving in space when cortical functions for blur discrimination are deferred.

Tadin proposes that the brain's ability to suppress irrelevant information applies to many processes beyond visual attention. Tadin assessed the correlation of cortical state with the strength of suppressive mechanisms on subjects including the elderly and individuals with schizophrenia, both of which are associated with GABAergic deficits (Tadin, 2015), (Tadin, Kim, Doop, Gibson, Lappin, and Blake, 2006). Populations such as children and those with major depression, and autism show relatively limited suppressive mechanisms (Golomb, McDavitt, Ruf, Chen, Saricicek, Maloney, Hu, Chun, and Bhagwagar 2009),

(Lewis, Sekuler, and Bennet, 2008) (Aurora and Wilkinson, 2007). On the other hand, migraines, considered to be a hyper-excited cortical state, show increased center-surround suppressive mechanisms for drifting stimuli (Battista, Badcock, and McKendrick, 2011).

Burr reports physical limitations of suppressive mechanisms, suggesting that the stimuli must be presented for at least 100ms (Burr et al. 1986). In our study, the 500ms presentation time exceeds the time necessary for a potential suppression of edge blur to occur. Additionally, the 500ms presentation time greatly exceeds the time constant necessary for backward masking. Marinovic et al., observed the strongest asymmetric sharpening when an image's trailing edge follows the leading edge by ~60ms (Marinovic et al., 2013). They suggested that an active inhibitory mechanism like backward masking could explain this behavior. An inhibitory suppressive mechanism may be in effect in our experiment, however, it is unlikely that it is due to a masking process enacted by the leading edge of the stimulus.

Lappin reports that effects of spatial suppressive mechanisms diminished with decreasing stimuli velocity and were absent entirely absent at velocities less than 1 degree per second (Lappin, Tadin, Nyquist, and Corn, 2009). In our experiment, we first test for motion asymmetry with speeds of 0.5 degree per second versus 2.0 degrees per second. While we do note a limited presence of motion sharpening at 0.5 degrees per second, the effect is much more significant at the faster velocity. Similarly, stereoscopic motion-in-depth sharpening is more significant at a relative speed of 2.0 degrees per second than it is at 0.5 degrees per second. This significant sharpening was expected for the higher velocity

considering significant sharpening was previously noted by McCormack et al (McCormack et al., 2014).

Our monocularly edge-matched target experiment replicates the critical findings of McCormack et that motion sharpening for stereoscopic motion-in-depth is relatively stronger than for lateral motion having the same retinal image velocities (McCormack et al., 2014). This finding supports McCormack et als.' assertion that the stronger motion sharpening observed in stereoscopic motion-in-depth must originate in the visual processes of the brain, and is not just a product of ocular image motion sharpening asymmetries arising at a peripheral level (e.g., retinal ganglion cells) (McCormack et al., 2014). This assertion is consistent with reports of suppressive mechanism at the cortical level by Anderson and Tadin (Anderson et al., 1987) (Tadin, 2015).

The results of Experiment 3 surprised us because we considered asymmetric edge sharpening and binocular motion sharpening to be separate, additive effects. The presence of asymmetric trailing edge sharpening was confirmed in Experiment 1. An additional, symmetrical sharpening effect was noted in Experiment 2, when asymmetric sharpening was neutralized in the ocular images. We predicted that additional sharpening would occur if both mechanisms functioned simultaneously. If they were additive, the relative strength of stereoscopic sharpening versus lateral sharpening in Experiment 3 would have been greater than in Experiment 2. Instead, overall sharpening in Experiment 3 was not significantly different from Experiment 2.

This finding leads us to believe that there may be an overall ceiling effect on motion sharpening or that the perception of asymmetric sharpening is negated in the process of

binoculary fusing the components of the three dimensional image. Perhaps this is yet another example of suppressive mechanisms in play, attempting to parse out information from a scene.

6.2 Complications and Limitations of the Study

Although our study population of 9 subjects is relatively small, the within-subjects design and repeats of all conditions allowed us to detect moderate and large differences of sharpening between conditions and between subjects. Each subjected observed 960 trials consisting of all possible parameter combinations. As mentioned earlier, steps were taken to limit the effects of practice on the results by randomizing the order of experiments, nullifying the individual subject's improved performance in making blur judgments on their final experiment.

The LCD display utilized in the experiment may have had a small effect in the degree of sharpening evidenced in our study. This effect, however, would have been to limit the amount of sharpening noted if present. Sylvain Tourancheau et al. note that LCD displays utilize a sample-and-hold behavior which causes objects to remain static on the screen for the full duration of a frame (8msec), while the viewer's eyes are still in smooth pursuit across the screen. The transient discrepancy in image versus eye location causes a small degree of motion blur (Tourancheau et al., 2009). A calculation of the amount of LCD motion smear demonstrates a non-significant effect on our study. If the eye is moving at the maximum velocity of of 2°/sec (120'/sec), the image is smeared 0.96' (less than one pixel) over 8msec. In other words, screen persistence is so small on our screen, in our conditions, that it could

not possibly be detected. Any smear must be visual. We were able to find a significant degree of motion sharpening even with the negligible effect of LCD motion blur.

Despite these limitations, we are now aware that the suppressive mechanisms of asymmetric motion sharpening and stereoscopic motion-in-depth sharpening exist, and may have a role in compensating for aberrant blur associated with accommodative convergence mismatch.

6.3 Applications for Future Research

The results from our experiment demonstrate the presence of motion sharpening in a setting of constant vergence. The subject fixates on a point in the plane of the screen for the duration of the trials. Stereoscopic stimuli can also generate depth while stimulating vergence. The oculomotor system may provide yet another mechanism for motion sharpening with stereoscopic motion in depth. It is already well established that suppressive mechanisms are in effect during saccades. The visual system will suppress visual information during jumps in fixation to eliminate motion blur and the discontinuity during the gap in perception.

In a study of motion smear during vergence and pursuit tracking, Bedell observed comet-like tails trailing behind luminous spots. Bedell's study compared luminous small spot stimuli moving at a constant retinal image velocity in darkness when subjects were either tracking the spot or fixating at a central point. Bedell was able to demonstrate reductions in luminous smear with changes in convergence with the greatest smear occurring when vergence was fixed. This finding supports the idea of "motor sharpening," an additional

form of sharpening with stereoscopic motion in depth (Bedell). It is not clear that Bedell's observation is valid for motion sharpening of relatively large, physically blurred objects in a photopic environment.

In an upcoming study, we will evaluate stereoscopic sharpening in setting of fixed versus changing vergence for both foveal and parafoveal stimuli. In each condition retinal image velocity will be constant. This experiment will test for signals, potentially associated with vergence corollary discharge signals, that serve to perceptually sharpen motion stereopsis images.

The presence of motor sharpening may or may not be additive with the process of motion sharpening noted in our previous experiment. We have found that asymmetric sharpening and symmetric sharpening in combination, do not provide a significantly different amount of overall sharpening. Perhaps the same is true to motor sharpening and motion sharpening. It may be the case however, that these two mechanisms are responsible for suppressing the aberrant blur of accommodative convergence mismatch in binocularly normal individuals. A failure of these mechanism may explain many viewers' aversion to 3D films and devices. The study of visual discomfort with 3D displays continues with further study of blur and suppressive mechanisms with stereoscopic stimuli.

CHAPTER 7

APPENDIX

Subject Screening Results											
SUBJECT	Age	Correction Right Eye	Correction Left Eye	Stereo Acuity	DVA Right Eye	DVA Left Eye	Cover Test	Far VG	Near VG	Accom. Amplitude	Near Point of Convergence
ACM	24	None	None	20"	20/20	20/20	Ortho	1xp	2xp	10D	To the nose
BHC	24	-0.50	-0.50	10"	20/20	20/20	Ortho	1ep	3xp	10D	To the nose
DJS	25	-1.00 – 0.50x115	-0.75 – 1.00 x 065	20"	20/20	20/20	Ortho	2xp	6xp	9D	5cm
GGL	25	-1.00 – 0.25 x 180	-1.50 – 0.25 x 180	20"	20/20	20/20	Ortho	1.5xp	6xp	10D	To the nose
JCL	23	-0.25 – 0.75 x 165	-0.25 – 0.75 x 015	20"	20/15	20/15	Ortho	2ep	2ep	11D	6cm
JKF	23	– 4.75	– 4.50	10"	20/15	20/15	Ortho	1xp	1.5ep	8D	4cm
JSM	25	-3.50 – 0.25 x 015	-3.25 – 0.50 x 175	20"	20/20	20/20	Ortho	2xp	3xp	9D	To the nose
MMC	23	+1.00 – 1.50 x 011	+0.75 – 1.50 x 165	16"	20/20	20/20	Ortho	2xp	2xp	10D	6cm
SLM	33	None	None	20"	20/20	20/20	Ortho	2xp	3xp	10D	To the nose

Table (1): 9 subjects (4 male, 5 female) that completed Experiments 1, 2, and 3. Listed are the subjects, aged 23-33 years old with refractive correction ranging from plano to -3.50 diopters sph and -1.50 diopters cylinder. Stereoacuity, measured in seconds of arc, ranged from 20" to 16". Distance visual acuity (DVA) was measured to be 20/20 or better in all subjects. All subjects were orthophoric without tropia, with phorias measues in prism diopters by the Von Graefe technique (VG) ranging from 2 esophoria (ep) to 3 exophoria (xp). Amplitude of accommodation ranged from 8 diopters to 11 diopters and near point of convergence values ranged between 6cm and 0cm (to the nose).

7.1 Purpose of the Pilot Experiment

The psychophysical method best suited for finding the perceptual match values in this study was not immediately apparent. McCormack et al. (2104) measured motion sharpening with a QUEST adaptive staircase technique that often displayed a bias to overestimate the blur of the blurred 'moving' target in a blur matching paradigm, even when its velocity was set to zero. Finding no programming bugs to explain this behavior they began to suspect that the QUEST algorithm might not be optimal for blur matching psychophysics. We launched a pilot study to compare QUEST with Best PEST, an alternative adaptive staircase procedure. The pilot study was performed on 6 subjects, five of which continued to complete Experiments 1, 2, and 3.

QUEST assumes that the psychometric function is asymmetrical, with the shape of a Weibull function, while Best PEST assumes that the psychometric function is a symmetrical logistic function. We speculate that the blur discrimination psychometric function is symmetrical like the logistic function, and that the use of QUEST with its asymmetric Weibull function may have caused a match blur bias. In this pilot study we collected blur discrimination data by a constant stimulus method, which does not assume the shape of the psychometric function, and then fitted that data with Weibull and logistic curves. We answered three questions with these fits: (1) Is the blur discrimination psychometric function more similar to a logistic shape or a Weibull shape, (2) Do the Weibull curve fits plotted on linear blur axes cause a match blur overestimation relative to the logistic fits, and (3) If the answer to the second question is 'yes', then does fitting our blur discrimination data with a Weibull curve on a log blur axis eliminate the match blur bias?

Six subjects were enrolled in the pilot study to discover which of the two methods was most suitable for our experimentation. These six subjects participated in the three sessions of the full experiment. Stimuli were of the same type as Experiment 1, utilizing the same parameters. In all trials, the trailing edge was a constant value of 42 degrees of blur with the leading edge blur adjusted to match the trailing edge blur. The data were analyzed with either a logistic function, a Weibull function on a linear blur axis ('linear Weibull'), and a Weibull function on a log blur axis ('log Weibull') to assess for the method that provides the best fit of the subjects' responses.

7.2 Procedure for the Pilot Experiment

The six subjects viewed monocular blurry bar stimuli moving leftward or rightward at 1 degree per second. The blur of the leading edge was variable, while the trailing edge was maintained at a constant 42 degrees of blur. Using a constant stimulus method, the leading edge was presented with 9 different blur steps of 3 degree increments. Each blur step was presented 20 times over the course of the pilot experiment. The subject responds to the question, "Was the leading edge blurrier than the trailing edge?" Once responses were recorded, Weibull and logistic curves were fit to the data by a Levenberg-Marquardt procedure in the LabView software. The Levenberg-Marquardt routine provided best fit values for logistic, linear Weibull, and log Weibull functions. The lowest chi value representing best fit decided which function was most appropriate psychophysical method for our experiment.

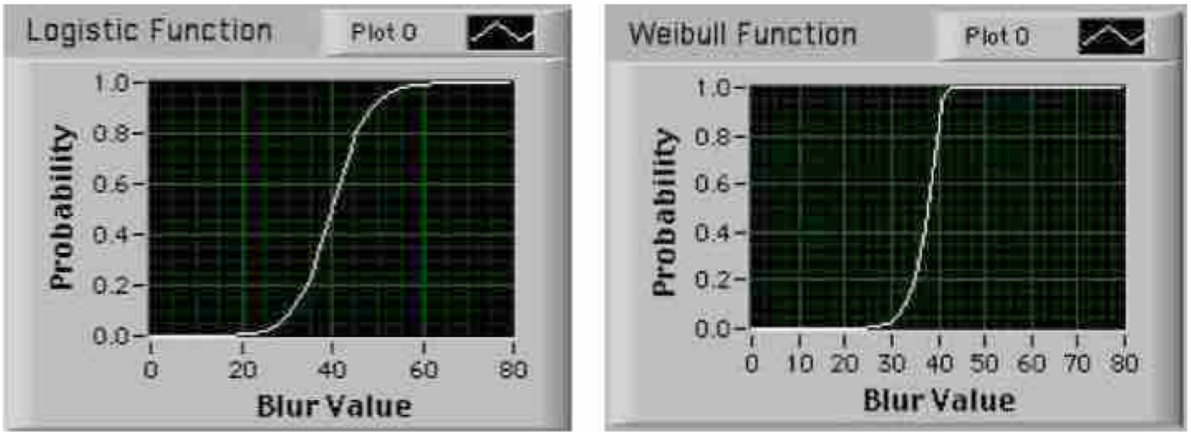


Figure (16): Examples of Logistic (left) and Weibull (right) curves plotted on linear axes. The logistic curve is symmetric about its midpoint while the Weibull curve rises relatively steeply at higher probabilities. The logistic function took the form y=1/(1+exp((x-a)/b)+1). The Weibull function took the form y=1-exp(-10exp(b*(x+a)).

7.3 Analysis of the Pilot Study Data

A logistic function best fit the data from the six pilot subjects, although the results did not differ greatly from linear and log Weibull functions. In 12 of 12 curve fits, a logistic function provided the lowest χ^2 value ($t = 3.16$, $p = 0.010$, $df = 10$). Overall, the logistic fit associated with the Best PEST psychophysical method appeared to be best suited for this experiment.

To answer the second question, subject responses were plotted for both leftward and rightward motion directions. The plots were fit with logistic, linear Weibull, and logistic Weibull functions. Two paired t-tests were conducted for leftward and rightward match values, using Bonferroni analysis ($p < 0.025$) to control for Type 1 error. For 11 of 12 plots, a logistic function provided smaller match values than the linear Weibull functions. Match

values obtained through logistic fits were significantly lower than Weibull fits for both leftward ($p < 0.001$) and rightward motion ($p < 0.021$). This finding supports McCormack et al's previous report of erroneously large QUEST match values when a linear Weibull fit was applied (McCormack et al., 2014).

To answer our third question, and address Watson and Pelli's claim that Weibull functions are best suited for data presented on a log stimulus axis (Watson and Pelli, 1983), match derived from the log Weibull fits were compared to match values derived from logistic fits on a linear blur axis. There was now no significant difference in mean match blurs beteen logistic and log Weibull match values ($t = 0.63$, $p = 0.54$, $df = 11$).

LITERATURE CITED

Allman, J. Miezin F, McGuinness E. (1985). Stimulus specific responses from beyond the classical receptive field: neurophysiological mechanism for local-global comparisons in visual neurons. *Annual Review of Neuroscience*. 8: 407-430

Anderson CH, Van Essen DC. (1987). Shifter circuits: a computational strategy for dynamic aspects of visual processing. *Proc Natl Acad Sci USA*. 84(17): 6297-6301.

Aurora SK, Wilkinson F. (2007). The brain is hyperexcitable in migraine. *Cephalgia*. 27(12): 1442-1453

Aznar-Casanova JA, Romeo A, Gomez AT, Enrile PM. (2017). Visual fatigue while watching 3D stimuli from different positions. J Optom. 10(3):149-160.

Barlow HB. (1958). Temporal and spatial summation in human vision at different background intensities. *J Physiol*. 141: 337-350.

Battista J, Badcock DR, McKendrick AM. (2011). Migraine increases centra-surround suppression for drifting visual stimuli. *PLoS ONE*. 6(4): e18211.

Bedell HE, Chung S, Patel S. (2004). Attenuation of perceived motion smear during vergence and pursuit tracking. *Vis Res*, 44:895-902.

Bex PJ, Edgar GK, Smith AT. (1995). Sharpening of drifting, blurred images. *Vision Res*. 35(18): 2539-2546.

Brooks, KR. (2017). Depth Perception and the History of Three-Dimensional Art: Who Produced the First Stereoscopic Images? *I-Perception*, *8*(1), 2041669516680114.

Burr D. (1980). Motion smear. *Nature*. 284(5752): 164-165.

Burr DC, Ross J. (1982). Contrast sensitivity at high velocity. *Vision Research*. 22: 479-484.

Burr DC, Ross J, Morrone MC. (1986). Seeing objects in motion. *Proc R Soc Long B Biol Sci*. 227(1247): 249-265.

Burr DC, Morgan MJ. (1997). Motion deblurring in human vision. *Proc Biol Sci*. 64(1380): 431-436

Chen S. Bedell HE, Ogmen H. (1995). A target in real motion appears blurred in the absence of other proximal moving targets. *Vis Res*. 35: 3215-3328.

Davidson RM, Bender DB. (1991). Selectivity for relative motion in the monkey superior colliculus. *Journal of Neurophysiology*. 65(5): 1115-1133.

Eifuku S, Wurtz RH. (1998). Response to motion extrastriate area MSTI: center-surround interactions. *Journal of Neurophysiology*. 80(1). 282-296.
Fawcett SL, Wang YZ, Birch EE. (2005). The Critical Period for Susceptibility of Human Stereopsis. *Investigative Ophthalmology & Visual Science*, 46: 521-525

Georgeson MA. (1987). Temporal properties of spatial contrast vision. *Vis Res*. 25: 765-780.

Golomb JD, McDavitt JR, Ruf BM, Chen HI, Saricicek A, Maloney KH, Hu J, Chun MM, Bhagwagar Z. (2009). Enhanced visual motion perception in major depressive disorder. *J Neurosci*. 29(28): 9072-9077.

Gorea A, Tyler CW. (1986). New look at Bloch's law for contrast. *J Opt Soc Am A*. 3: 52-61

Hammett ST, Georgeson MA, Gorea A. (1997). Motion blur and sharpening: temporal smear and local contrast non-linearity. *Vision Res*. 38(14): 2099-2108.

Hammet ST. (1997). Motion blur and motion sharpening in the human visual system. *Vis Res*. 37: 2505-2510.

Held RT, Hui TT. (2011). A Guide to stereoscopic 3D displays in medicine. *Academic Radiology*, 18(8): 1035-1048.

Hoffman DM, Girshick AR, Akeley K, Banks MS. (2008). Vergence-accommodation conflicts hinder visual performance and cause visual fatigue. *J Vis*. 8(3):33.1-30.

Howarth PA. (2011). Potential hazards of viewing 3-D stereoscopic television and cinema: a review. *Ophthalmic Physiol,* 31(2): 111-122.

Jones HE, Wang W, Stillito AM. (2002). Spatial organization and magnitude of orientation contrast interactions in primate V1. *Journal of Neurophysiology*. 88(5): 2796-2808.

Kollin J, Hollander Ari. (2007). Re-engineering the Wheatstone stereoscope. *The international society for optics and photonics* website. http:// http://spie.org/newsroom/0673-re-engineering-the-wheatstone-stereoscope?SSO=1. March 20, 2007. Accessed January 3, 2018.

Lappin JS, Tadin D, Nyquist JB, Corn AI. (2009) Spatial and temporal limits of motion perception across variations in speed, eccentricity, and low vision. *Journal of Vision*. 9: 1-14

Legge GE. (1978). Sustained and transient mechanism in human vision: spatial and temporal properties. *Vis Res*. 18: 69-81.

Lewis T, Sekuler A, Bennett P. (2008). Psychophysical measurements of surround suppression in 5-year-olds. *Journal of Vision*. 8(6): 388-388.

Liebermann HR, Pentland AP. (1982). Microcomputer-based estimation of psychophysical thresholds: The Best PEST. *Behavioral Research Methods & Instrumentation*. 14(1): 21-25.

MacCurdy E. (1956). *The notebooks of Leonardo Da Vinci*. London: Jonathan Cape (2): 230

Madigan R, Williams D. (1987). Maximum-likelihood psychometric procedures in two-alternative forced choice: Evaluation and recommendations. *Percep & Psychophys*. 42(3): 240-243.

Marinovic W, Arnold DH. (2013). An illusory distortion of moving form driven by motion deblurring. *Vision Res*. 88: 47-54.

McCormack G, Van Cura J, Bex P. (2014). Neural Sharpening of Images Moving in Stereoscopic Depth. *Invest Ophthalmol Vis Sci*. 55:ARVO E-Abstract 3002.

Melnick MD, Harrison BR, Park S, Bennetto L, Tadin D. (2013). A strong interactive link between sensory discriminations and intelligence. *Curr Biol*. 23(11): 1013-1017

Moore S, McCormack G. (2015). Motion Sharpening of Looming Vertical Bars. *Invest Ophthalmol & Vis Sci*. 55: ARVO E-abstract #2928.

Newton, Sir Isaac. (1730) *Opticks*. 536

Paakkonen AK, Morgan MJ. (1994). Effects of motion on blur discrimination. *J Opt Soc Am A*. 11:992-1002.

Shibata T, Kim J, Hoffman DM, Banks MS. (2011). The Zone of comfort: Predicting visual discomfort with stereo displays. *J Vis*. 11(8): 11.

Tadin D, Lappin JS, Gilroy LA, Blake R. (2003). Perceptual consequence of centre-surround antagonism in visual motion processing. *Nature*. 424(6946): 312-315.

Tadin D, Kim J, Doop ML, Gibson C, Lappin JS, Blake R. (2006). Weakened center-surround interactions in visual motion processing in schizophrenia. *Journal of Neuroscience*. 26(44): 11403-11412.

Tadin D. (2015). Suppressive mechanisms in visual motion processing: From perception to intelligence. *Vision Res*. 115(A):58-70

Taylor CP, Bex PJ. (2015). On the number of perceivable blur levels in naturalistic images. *Vision Research.115*: 142–150.

Taylor MM, Creelman CD. (1967). PEST: Efficient estimates on probability functions. *Journal of the Acoustical Society of America*. 41:782-787.

Thompson, P. (1982). Perceived rate of movement depends on contrast. *Vision Research*. 22: 377-380.

Tourancheau S, Le Callet P, Brunnstrom K, Andren B. (2009). Psychophysical study of LCD motion-blur perception. *Human Vision and Electronic Imaging*. 14(1): 7240-7251

Turnbull PRK, Phillips JR. (2017). Ocular effects of virtual reality headset wear in young adults. *Sci Rep*. 7(1): 16172.

Watson A, Pelli DG. (1983). QUEST: A Bayesian adaptive psychometric method. *Percep & Psychophys*. 33(2): 113-120.